Aeromechanics Investigation of Tiltrotor Transition Maneuver

Hyeonsoo Yeo
US Army Combat Capabilities Development Command
Aviation & Missile Center
Aviation Development Directorate
Ames Research Center, Moffett Field, CA, USA

Hossein Saberi
Advanced Rotorcraft Technology, Inc.
Sunnyvale, CA, USA

Graham Bowen-Davies*
Science and Technology Corporation
Ames Research Center, Moffett Field, CA, USA

ABSTRACT

Aeromechanics analysis is performed using the comprehensive analysis code RCAS (Rotorcraft Comprehensive Analysis System) to study the transient conversion maneuver of a tiltrotor. The analytical model is based on the XV-15 research tiltrotor aircraft in size and dynamic characteristics. A generic (not representative of XV-15) tiltrotor control system is developed to simulate conversion maneuver. The calculation begins with a trim analysis at hover, which is followed by the conversion maneuver. During the maneuver analysis, the pilot control model is activated to fly the aircraft following a desired airspeed profile and zero altitude change. Time histories of vehicle dynamics, rotor controls, rotor flapping, rotor performance and blade structural loads are investigated for various transient conversion maneuver flight conditions. The aircraft longitudinal acceleration is larger for the faster conversion (shorter conversion time) and for the higher cruise speed (conversion end speed). The aircraft acceleration during the transient maneuver has a significant influence on the rotor performance and loads.

INTRODUCTION

There has been a growing need for significant increases in cruise speed and range capabilities over what conventional helicopters can achieve for both civil and military applications. Tiltrotor aircraft enable both helicopter-like hover capabilities and fixed-wing-like high speed cruise capabilities that increase range and endurance over traditional helicopters.

Tiltrotor aircraft are becoming increasingly common. A very successful demonstration of tiltrotor technology with the XV-15 in the 1980s prompted the development of the Bell-Boeing V-22 Osprey tiltrotor, which was fielded in the late 2000s (Ref. 1). The Leonardo AW609 is currently undergoing certification flight testing (Ref. 2). As part of the US Army's Joint Multi-Role Technology Demonstrator program, Bell is developing the V-280 Valor (Ref. 3).

*Currently at Kitty Hawk Corporation

Presented at the 45th European Rotorcraft Forum, Warsaw, Poland, September 17–20, 2019.

The accurate computation of blade loads and airframe loads during transient maneuver is one of the most important aeromechanics tasks that must be accomplished in order to define the flight envelope of a rotorcraft and size rotor dynamics components and fixed systems controls (Refs. 4–7). Designs based on inaccurate loads often require a costly modification, additional testing, weight penalties, and overall performance degradation of an aircraft. Significant difficulty arises for new configurations, where there are no previous flight test data from rotorcraft which are dynamically and aerodynamically similar to the configuration of interest. A risk mitigation step in the design and development of tiltrotors is the use of an analysis tool that can properly model the coupled rotor-airframe-control system through transient maneuvers.

There has been much aeromechanics research on tiltrotor aircraft (Refs. 8–15) through analyses. These analyses have included various hub types, rotor geometries, analysis tools and fidelity and they have considered rotor performance, loads and aeroelastic stability.

The transition maneuver of the full vehicle, in which the rotor experiences both edgewise flight in hover and low-speeds and axial flow in cruise, creates a unique and interest-

ing aeromechanics environment that has not been fully investigated with rotorcraft comprehensive analyses. Previous analytical research on aspects of tiltrotor transition has mostly focused on rotor-only analyses of quasi-steady conditions in the transition region. Rotorcraft comprehensive analysis codes have been used to analyze various transient maneuver flight conditions (Refs. 5, 7, 16, 17).

The present paper studies the aeromechanics of a tiltrotor that maneuvers (time marching transient analysis) through transition from hover to high speed cruise using the comprehensive analysis code RCAS (Rotorcraft Comprehensive Analysis System) (Ref. 18). The analytical model is based on the XV-15 (Ref. 19) in size and dynamic characteristics, as shown in Fig. 1. The XV-15 is a tiltrotor research aircraft that was developed by Bell. The aircraft was used to demonstrate the flight envelope and capabilities of tiltrotor aircraft. The present model has an accurate representation of gimballed rotors of the XV-15. However, some assumptions were made to simplify the model and analysis. A simple pilot model is developed in order to enable the model to perform a reasonable conversion maneuver based on altitude and airspeed schedule commands. Transient response time histories of vehicle dynamics, rotor controls, rotor flapping, rotor performance and blade structural loads are investigated.

In summary, the purpose of this paper is two fold: 1) to develop a generic tiltrotor configuration similar to the XV-15 with a control system to perform transient conversion maneuver and 2) to investigate vehicle dynamics, rotor controls, rotor flapping, rotor performance and blade structural loads during conversion flight.

DESCRIPTION OF ANALYTICAL MODEL

The comprehensive rotorcraft analysis code RCAS is used for modeling and analysis of tiltrotor conversion. Figure 2 shows the RCAS tiltrotor model used for the present study. This section describes how the RCAS generic tiltrotor model based on the XV-15 is developed to perform a conversion maneuver analysis from hover to cruise in this study. Detailed dynamic properties of the XV-15 gimballed rotor and fuselage and limited test data are available in Refs. 20 to 23.

The current RCAS tiltrotor configuration consists of structural, aerodynamic, and control system models. The overall structural model is composed of three subsystems: fuselage, left rotor, and right rotor. The fuselage subsystem consists of several primitive structures that model the basic fuselage, left and right wings, two nacelles, two vertical tails, and a horizontal tail. Rigid body mass elements model the inertial and gravitational loads of all the components of the fuselage subsystem. The wings are modeled with rigid bar elements oriented to provide dihedral and forward sweep. Control hinge elements at the wing tips rotate the nacelles. A rigid bar element for each nacelle connects the control hinge to its rotor. Each rotor is composed of a gimbal and three blades. The gimbal is modeled as a constant velocity joint. Each blade is modeled with 12 elastic nonlinear beam elements and the pitch bearing, pitch link and pitch horn are modeled with rigid bar and spring elements. The RCAS dynamic model for the rotor was obtained from a CAMRAD (Comprehensive Analytical Model of Rotorcraft Aerodynamics and Dynamics) II model of the XV-15 (Ref. 21).

The aerodynamic model is composed of seven aerodynamic supercomponents: right and left rotor, fuselage, main wing, horizontal tail, and right and left vertical tails. The fuselage is modeled with linear aerodynamic coefficients such that lift, drag, and pitch moment are computed as functions of dynamic pressure. The main wing is modeled with 25 aerodynamic segments. The 6 inboard and 8 outboard segments model the flap and aileron, respectively, for control system inputs. The horizontal tail is made up of 11 aerodynamic segments and the 8 inboard segments model the elevator for control system inputs. Each section of the vertical tail is modeled with 10 aerodynamic segments and rudder is incorporated for control system inputs. The wing and tails are modeled with linear aerodynamic coefficients for lift and drag coefficients (no pitching moment). Each blade is modeled with 18 aerodynamic segments. The lift, drag, and pitching moment on each aerodynamic segments are calculated using airfoil characteristics from C81 lookup tables provided in Appendix A of Ref. 22. Linear unsteady airloads include classical quasi-steady Theodorsen theory. Finite state dynamic inflow model is used to calculate rotor wake flowfield. The model includes time dependent characteristics for loading distribution defined by multiple azimuthal harmonics and radial mode functions. For the present analysis, 6 radial polynomials and 6 harmonic functions (6 X 6) are used. No inflow model is used for the wing and tails and no interference effects are included among the aerodynamic supercomponents.

The present tiltrotor control system was modeled using the Control System Graphical Editor (CSGE). CSGE is a graphical user interface that contains an extensive library of linear and nonlinear elements such as transfer functions, gains, summing junctions, saturations, limiters, table lookups, filters, etc. It provides an intuitive graphical user interface (GUI) that allows users to draw control system block diagrams graphically. It also provides the capability for general, arbitrary arrangement and connection of the control system elements and interfaces with the rest of the model including couplings of the control system and structural models.

The present control model includes only the longitudinal dynamics of the aircraft due to symmetry. The longitudinal pilot model consists of the two control paths for the altitude and airspeed and a simple stability augmentation system. The function of the pilot model is to follow the input commands and fly the model through conversion in a simple manner. It uses airspeed and altitude commands as well as sensed actual values from the airframe dynamic response to reduce the differences between them.

The nacelle angle is prescribed as a nonlinear function of airspeed. Forward conversion from hover to airplane mode flight ends when the prescribed cruise speed is reached. In each case, the difference between the commanded and actual variables along with their integrals and derivatives are mixed

and gain scheduled and passed to the pilot longitudinal stick controls. The mixing and gain schedule of the feedback signals are chosen to represent simple pilot behavior.

The pilot longitudinal cyclic controls the rotor swashplate longitudinal cyclic and the elevators. In helicopter mode, the gain from the pilot longitudinal cyclic to the swashplate longitudinal cyclic is high. As the nacelles are tilted forward, the gain is reduced and at zero nacelle tilt in airplane mode there is no input to the swashplate longitudinal cyclic. Elevator effectiveness increases with airspeed such that in the airplane mode, pitch angle, and hence the aircraft vertical motion, are controlled by the elevator.

Figure 3 shows a simplified representation of the airspeed control system. It uses airspeed (AS) command and sensed actual airspeed (calculated from the aircraft dynamic response) and tries to reduce the differences between the two quantities. At low speed, longitudinal cyclic is used and at high speed collective is used to maintain the commanded airspeed.

Figure 4 shows a simplified representation of altitude command and hold system. It used altitude (Alt) command and sensed actual altitude calculated from the aircraft dynamic response and try to reduce the differences between the two quantities. It also uses sensed actual vertical speed. At low speed, collective is used and at high speed elevator is used to maintain the commanded altitude.

Figure 5 shows that aircraft pitch (θ) and pitch rate (q) are used as a simple Stability Augmentation System (SAS).

The control system in this model does not represent the XV-15 tiltrotor control system, but was designed for the present purpose to simulate conversion maneuvers from hover to cruise in a reasonable manner. There was no attempt to optimize the pilot model nor to optimize the control mixing of helicopter and fixed-wing controls.

RESULTS AND DISCUSSION

Tiltrotor conversion maneuver analysis is conducted using the comprehensive analysis RCAS and the calculated results are presented here. This section shows transient response time histories of vehicle dynamics, rotor controls, rotor flapping, rotor performance and blade structural loads for various transient conversion maneuver flight conditions.

Analysis procedure

The transition maneuver analysis of the full vehicle is carried out from hover (90° nacelle angle) to cruise (0° nacelle angle). First, a trim analysis is performed to obtain control variables to find the equilibrium solutions for a steady state operating condition. During the trim analysis in hover, rotor collective and longitudinal cyclic and aircraft pitch attitude are used to trim aircraft vertical and longitudinal forces and pitch moment. Next, the conversion maneuver is performed as a nonlinear transient response in the time domain. During the maneuver analysis, the pilot model is activated to fly the aircraft attempting to follow a desired airspeed profile with zero altitude change. The transient conversion is followed by steady level flight cruise for several seconds. Figure 6 shows snapshots of the RCAS conversion maneuver for hover, conversion, and cruise.

Operating conditions are sea level standard and 589 RPM rotor speed. A 2.5° (144 steps per rotor revolution) azimuthal step size is used for the trim calculations. The time step used in the transient response calculation was 0.000707 second, which corresponds to 2.5 deg azimuth angle. The current RCAS analysis uses full finite element representation of the rotor blades (no modal reduction) and rigid (no elastic) airframe motions.

In this study, four conversion maneuver scenarios are investigated; 1) hover to 180 knots in 30 seconds (0.31 g), 2) hover to 210 knots in 30 seconds (0.37 g), 3) hover to 180 knots in 45 seconds (0.21 g), and 4) hover to 210 knots in 45 seconds (0.24 g).

The total simulation time, including the additional time after cruise was reached, is 37 and 54 seconds for the 30-second and 45-second conversions, respectively. This correspond to about 360 and 534 rotor revolutions.

Transient conversion maneuver analysis results

Representative results are presented in this subsection which includes conversion maneuver variables and controls as well as aeroelastic and dynamic response of the vehicle and rotor blades.

Aircraft response Figure 7 shows the time history of vehicle commanded and actual airspeed for the four conversion scenarios. The commanded airspeed increases linearly from hover to cruise (180 and 210 knots) in 30 and 45 seconds. Overall the actual aircraft airspeed follows the commanded airspeed profile very well. In general, the biggest differences occur at the beginning of the conversion maneuver when the aircraft try to gain airspeed from hover and at the end of the conversion maneuver when the aircraft transitions to cruise mode.

Figure 8 shows the time history of vehicle commanded and actual altitude change. Altitude command was zero throughout the entire maneuver. The results show that the altitude was very well maintained initially, especially for the slower maneuver (45 seconds) cases. As the aircraft pitch increases (will be shown later), the altitude also increases. About 70 ft altitude increase is observed toward the end of the conversion maneuver.

Figure 9 shows the aircraft acceleration in longitudinal and vertical directions. The longitudinal acceleration is the time derivative of the actual airspeed shown in Fig. 7. The vertical acceleration is the second derivative of the actual aircraft altitude change shown in Fig. 8. Although the airspeed and altitude appear to vary smoothly, the acceleration fluctuates. The vertical acceleration increases from zero in hover to around 0.3 g at the beginning of the conversion and decreases from

around 0.3 g to zero at the end of the conversion. One interesting observation is the increase in acceleration between 22 and 30 seconds for the 30-second conversion cases and between 35 and 45 seconds for the 45-second conversion cases. The increase in acceleration has a significant influence in rotor performance and loads, shown later.

Figure 10(a) shows the nacelle angles. The present control system uses airspeed error (difference between actual and commanded values) and its integral to tilt the nacelle in addition to the scheduled angle (also shown in the figure). This feedback helps to reduce the airspeed error beyond the response to longitudinal cyclic. The sharp drop in the nacelle angle around the beginning of the maneuver is due to this feedback. Because the actual speed is lower than the commanded airspeed at the beginning of conversion (Fig. 7), the aircraft tried to accelerate by tilting nacelle forward quickly. In addition, an actuator model with the bandwidth of 2 Hz was included in the control system to prevent unrealistic nacelle tilt rate.

Figure 10(b) shows the aircraft pitch attitude. Initially the aircraft pitch is reduced to accelerate from hover to catch up with the commanded airspeed. And then aircraft pitches up to reduce airspeed overshoot. As the aircraft altitude increases, the control system reduces the aircraft pitch.

Rotor controls Figure 11 shows the controls used for the present conversion maneuver flight. The high collective pitch at the end of the conversion is required as the rotors encounter high axial flow. At all airspeeds during the conversion the pilot collective control is higher than the hover collective. For steady level flight conditions, collective at low speeds is lower than that in hover. However, collective increases in the present conversion maneuver flight due to forward acceleration.

The longitudinal cyclic is more effective at low airspeed and behaves as in a conventional helicopter. At the beginning of the conversion, the longitudinal cyclic is used to control the airspeed. Near the end of the conversion, it is reduced to zero.

Rotor performance Figures 12(a) and 12(b) show the rotor thrust and power, respectively. For steady level flight conditions, rotor thrust is the highest in hover and decreases with airspeed as the wing generates more lift as airspeed increases. For the present maneuver analysis, rotor thrust increases at the initial conversion states to provide energy for forward acceleration shown in Fig. 9. As the acceleration is higher for the 30-second conversion cases than for the 45-second cases, rotor thrust increase is also higher for the 30-second conversion cases. The rotor thrust increase between 22 and 30 seconds for the 30-second conversion cases and between 35 and 45 seconds for the 45-second conversion cases follows the trends in acceleration. The biggest increase occurs for the 210 knot, 30 second case as the biggest acceleration change occurred. More power is also required for forward acceleration as shown in Fig. 12(b). The trend is very much in agreement with that of acceleration. As the aircraft longitudinal acceleration is larger for the faster conversion (shorter conversion time) and for the higher cruise speed (conversion end speed), the rotor power is also higher for the faster conversion and for the higher cruise speed.

Gimbal flap response Figure 13 shows the gimbal flapping responses during the conversion maneuver. The calculated coning angles do not vary much during the transient maneuver. However, it generally follows the rotor thrust variation, as expected. The longitudinal flapping angle variation is similar to the longitudinal cyclic angle variation. Although lateral cyclic angle is zero during the maneuver, the lateral flapping angle is not because of cross-coupling.

Blade structural loads Figure 14 shows the blade flap bending moments at the 9.1% radial location (just outboard of pitch bearing). The mean flap bending moment variation is similar to the vertical acceleration variation. The maximum oscillatory (peak-to-peak) flap bending moment occurs near the end of the conversion flight, which is also consistent with the vehicle acceleration.

Figure 15 shows the chord bending moments at the 9.1% radial location. The magnitude of the mean chord bending moment increases with time. The magnitude of oscillatory chord bending moment is much smaller than that of flap bending moment.

Blade torsion moments are not shown as they are much smaller than the bending moments shown here.

Alternative conversion strategy

The conversion strategies investigated in the present study show that the maximum rotor power occurs towards the end of the conversion where the acceleration jump up and the maximum power values are about 2 - 3 times of the hover power. In order to address this issue, an alternative conversion strategy is examined briefly in this subsection.

Instead of the conversion maneuver based on altitude and airspeed schedule commands, the alternative conversion strategy uses collective and elevator angle to achieve desired engine power (thus rotor power) and aircraft pitch. The new strategy shifts high acceleration to lower speed to reduce the rotor power increase.

Figure 16 shows aircraft dynamics and rotor performance results for the 210-knot in 30-second conversion case with the alternative conversion strategy. The nacelle is prescribed to tilt forward linearly. The airspeed increases very slowly at the beginning of the conversion and then increases almost linearly from 18 seconds into the conversion to the end. Although the altitude command and hold system is not used, the altitude change is less than 50 ft. The aircraft acceleration is higher at lower speed, but lower at higher speed than the baseline case shown in Fig. 9(b). And thus the rotor thrust increases at around 10 seconds into the conversion, but the rotor thrust increase between 22 and 30 seconds (Fig. 12(a)) is eliminated. The maximum rotor power is reduced about 400 HP (16 %) compared to the baseline case (Fig. 12(b)).

Various conversion flight strategies will be systematically investigated and better pilot control models will be developed in the future.

CONCLUSIONS

This paper investigates the aeromechanics of tiltrotor conversion maneuver using the comprehensive analysis code RCAS (Rotorcraft Comprehensive Analysis System). The analytical model is based on the XV-15 in size and dynamic characteristics. A generic (not representative of XV-15) tiltrotor control system is developed to simulate conversion maneuver. Time histories of vehicle dynamics, rotor controls, rotor flapping, rotor performance and blade structural loads are investigated for various transient conversion maneuver flight conditions.

From this study the following conclusions are obtained:

1) A generic tiltrotor control system is developed to simulate transient conversion maneuver using airspeed and altitude commands. Overall, the actual aircraft airspeed follows the commanded airspeed profile very well and the altitude is well maintained at the beginning of the conversion and within 75-ft variation at the end of the conversion.

2) The aircraft acceleration in longitudinal and vertical directions is larger for the faster conversion (shorter conversion time) and for the higher cruise speed (conversion end speed). The acceleration profile has a significant influence in the rotor performance and loads during the conversion maneuver.

3) The rotor thrust increases at the initial conversion stage in order to provide energy for forward acceleration and the rotor thrust increase is larger for the faster conversion (shorter conversion time).

4) The rotor power is higher throughout the conversion maneuver than that in hover. As the aircraft longitudinal acceleration is larger for the faster conversion (shorter conversion time) and for the higher cruise speed (conversion end speed), the rotor power is also higher for the faster conversion and for the higher cruise speed.

5) The mean flap bending moment variation is similar to the vertical acceleration variation. The maximum oscillatory (peak-to-peak) flap bending moment occurs near the end of the conversion flight, which is also consistent with the vehicle acceleration.

6) An alternative conversion strategy is briefly examined to address the significant rotor power increase. About 400 HP (16 %) reduction in the maximum rotor power is achieved for the 210-knot in 30-second conversion case.

REFERENCES

[1]"V-22 Osprey 2010 Guidebook," NAVAIR PMA-275 Control Number 11-607, NAVAIR, 2011/2012.

[2]Dubois, T., "Leonardo presses ahead with AW609 certification program," https://www.verticalmag.com/news/leonardo-presses-ahead-aw609-certification-program/, retrieved on February 2019, published December 2016.

[3]Ehinger, R., Gehler, C., and Allen, S., "Bell V-280 Valor: A JMR-TD Program Update," American Helicopter Society 73rd Annual Forum Proceedings, Fort Worth, TX, May 9-11, 2017.

[4]Popelka, D. A., and Agnihotri, A., "Prediction and Alleviation of V-22 Rotor Dynamic Loads," American Helicopter Society National Specialists' Meeting on Rotorcraft Dynamics, Arlington, TX, November 13-14, 1989.

[5]Schillings, J., Roberts, B. J., Wood, T. L., and Wernicke, K. G., "Maneuver Performance Comparison between the XV-15 and an Advanced Tiltrotor Design," *Journal of the American Helicopter Society*, May 1990.

[6]Agnihotri, A., Idler, W., Milliken, R., and Singh, S., "V-22 EMD Design Loads Development Using V-22 FSD Flight Test Data," American Helicopter Society 50th Annual Forum Proceedings, Washington, D.C., May 11-13, 1994

[7]Corrigan, J. C., "Computation of Loads during Maneuvering Flight Using a Comprehensive Rotorcraft Code," American Helicopter Society National Specialists' Meeting, Fairfield Country, CT, October 4-5, 1995.

[8]Johnson, W., "Airloads and Wake Geometry Calculations for an Isolated Tiltrotor Model in a Wind Tunnel," 27th European Rotorcraft Forum Proceedings, Moscow, Russia, September 2001.

[9]Potsdam, M. A., and Strawn, R. C., "CFD Simulations of Tiltrotor Configurations in Hover," *Journal of the American Helicopter Society*, Vol. 50, (1), January 2005, pp. 82-94.

[10]Ho, J., and Yeo, H., "Assessing Calculated Blade Loads of the Tilt Rotor Aeroacoustic Model," *Journal of Aircraft*, Vol. 55, No. 3, May-June 2018.

[11]Yeo, H., Bosworth, J., Acree, C. W. Jr., and Kreshock, A. R., "Comparison of CAMRAD II and RCAS Predictions of Tiltrotor Aeroelastic Stability," *Journal of the American Helicopter Society*, 63, 022001 (2018).

[12]Johnson, W., "Dynamics of Tilting Proprotor Aircraft in Cruise Flight," NASA TN D-7677, May 1974.

[13]Shen, J., Singleton, J. D., Piatak, D. J., Bauchau, Q. A., and Masarati, P., "Multibody Dynamics Simulation and Experimental Investigation of a Model-Scale Tiltrotor," *Journal of the American Helicopter Society*, 61, 022010 (2016).

[14]Bowen-Davies, G., "Comparison of Vortex Wake, VVPM and CFD Aeromechanics Computations of the Boeing 222 Proprotor," American Helicopter Society 74th Annual Forum Proceedings, Phoenix, AZ, May 14-17, 2018.

[15]Tran, S., Lim, J., Nunez, G., Wissink, A., and Bowen-Davies, G., "CFD Calculations of the XV-15 Tiltrotor During Transition," Vertical Flight Society 75th Annual Forum Proceedings, Philadelphia, PA, May 13-16, 2019.

[16]Hwang, S., Lee, M. K., Kim, Y, and Kim, J. M., "Proprotor Load Evaluation in Collision Avoidance Maneuver of Tilt Rotor Unmanned Aerial Vehicle," American Helicopter Society Vertical Lift Aircraft Design Conference Proceedings, San Francisco, CA, January 18-20, 2006.

[17]Saberi, H. A., Khoshlahjeh, M., Ormiston, R. A., and Rutkowski, M. J., "RCAS Overview and Application to Advanced Rotorcraft Problems," AHS Fourth Decennial Specialists' Conference on Aeromechanics Proceedings, San Francisco, CA, January 21-23, 2004.

[18]Saberi, H., Hasbun, M., Hong, J. Y., Yeo, H., and Ormiston, R. A., "Overview of RCAS Capabilities, Validations, and Rotorcraft Applications," American Helicopter Society 71st Annual Forum Proceedings, Virginia Beach, VA, May 5-7, 2015.

[19]Maisel, M. D., Giulianetti, D. J., and Dugan, D. C., "The History of the XV-15 Tilt Rotor Research Aircraft: From Concept to Flight," The NASA History Series, NASA SP-2000-4517, 2000.

[20]Ferguson, S. W., "A Mathematical Model for Real Time Flight Simulation of a Generic Tilt-Rotor Aircraft," NASA CR-166536, September 1988.

[21]Acree, C. W. Jr., "An Improved CAMRAD Model for Aeroelastic Stability Analysis of the XV-15 with Advanced Technology Blades," NASA TM 4448, 1993.

[22]Acree, C. W., Jr., Peyran, R. J., and Johnson, W., "Rotor Design Options for Improving XV-15 Whirl-Flutter Stability Margins," NASA/TP-2004-212262, March 2004.

[23]Arrington, L., Kumpel, M., Marr, R., and McEntire, K., "XV-15 Tiltrotor Research Aircraft Flight Test Data Report," NASA CR 177406, June 1985.

(a) XV-15 Tilt Rotor Research Aircraft.

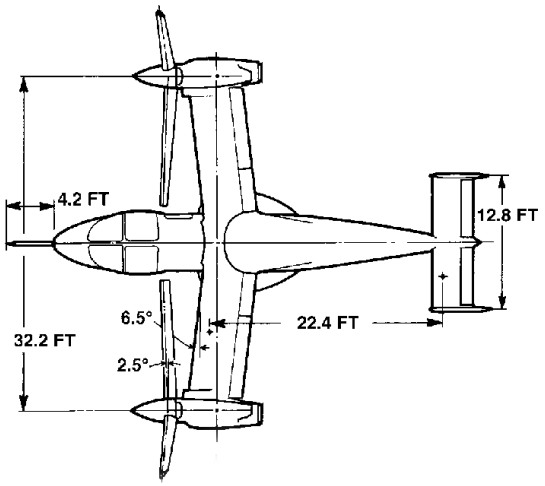

(b) Sketch plan view of XV-15 showing aircraft dimensions.

Fig. 1. XV-15 tiltrotor.

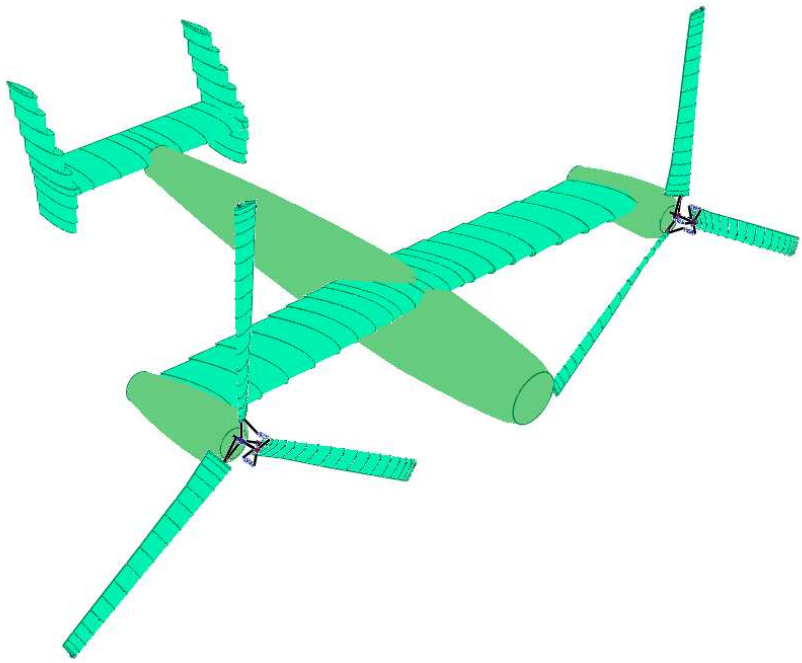

Fig. 2. RCAS tiltrotor model, based on the XV-15.

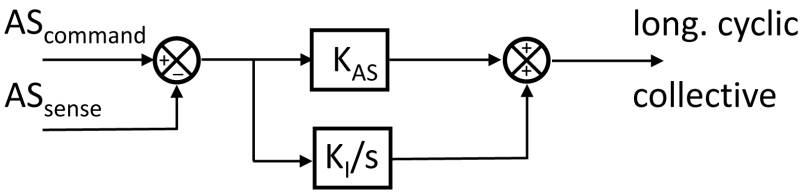

Fig. 3. Airspeed command and hold.

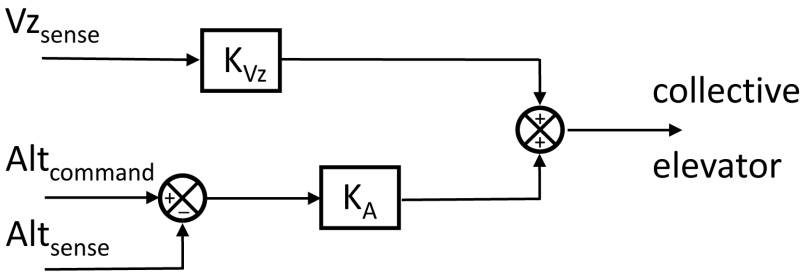

Fig. 4. Altitude command and hold.

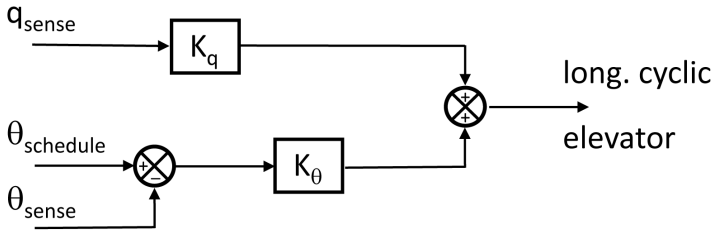

Fig. 5. Stability augmentation system.

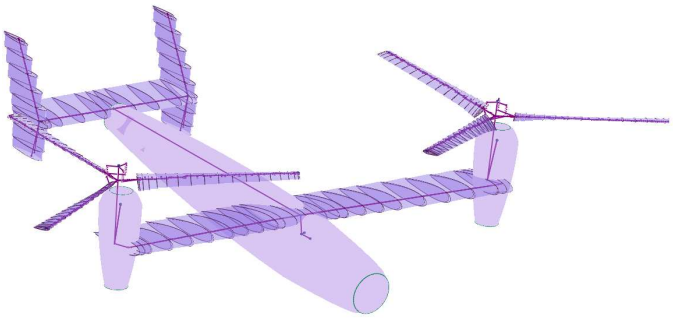

(a) Hover

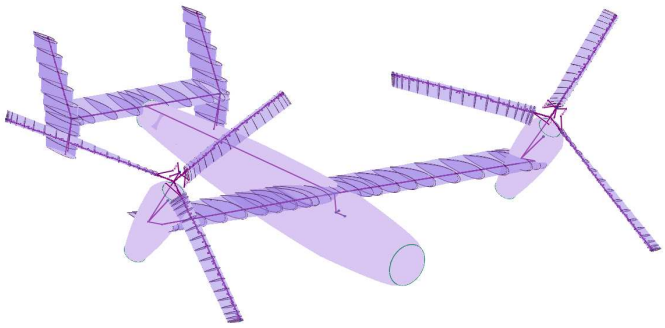

(b) Conversion

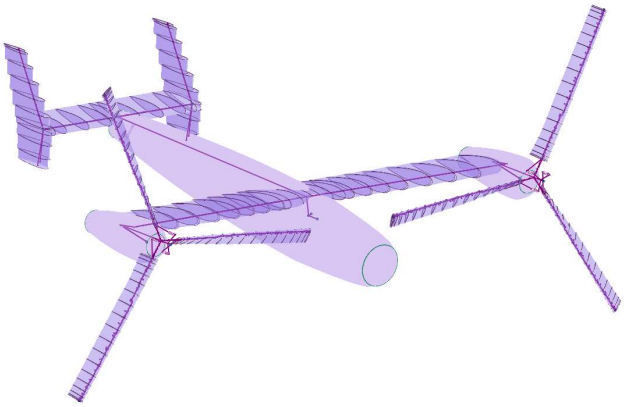

(c) Cruise

Fig. 6. Snapshots of RCAS conversion maneuver.

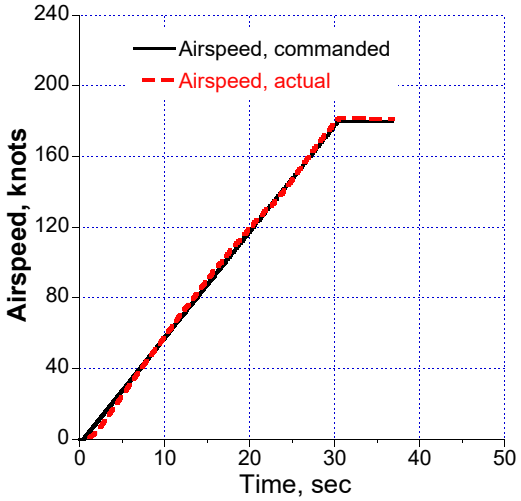

(a) 180 knot, 30 second

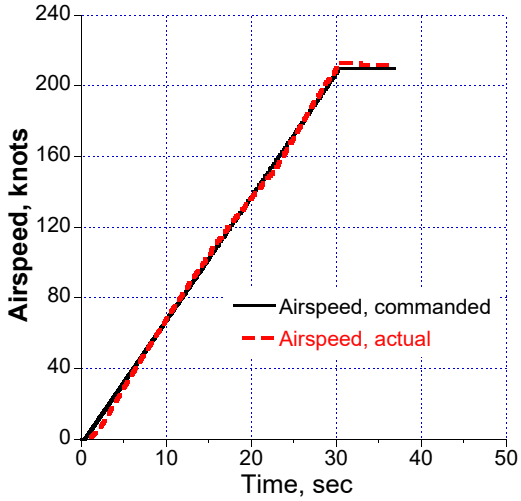

(b) 210 knot, 30 second

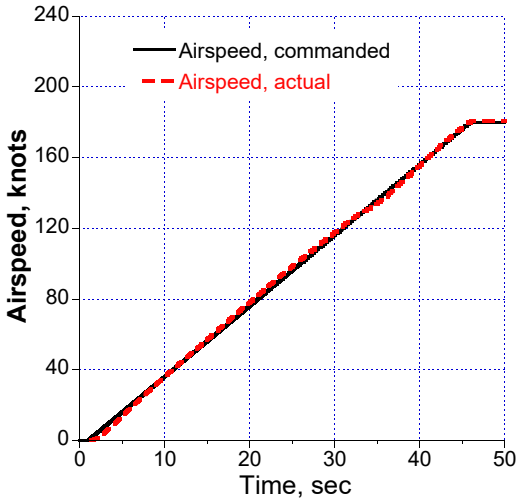

(c) 180 knot, 45 second

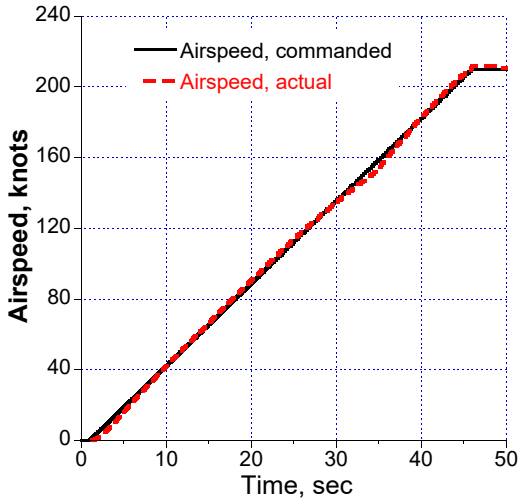

(d) 210 knot, 45 second

Fig. 7. Airspeed.

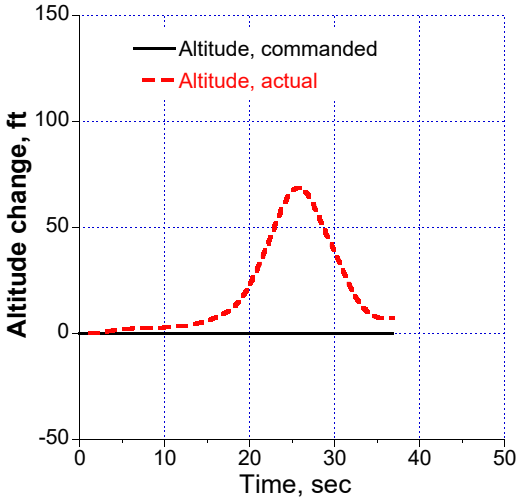

(a) 180 knot, 30 second

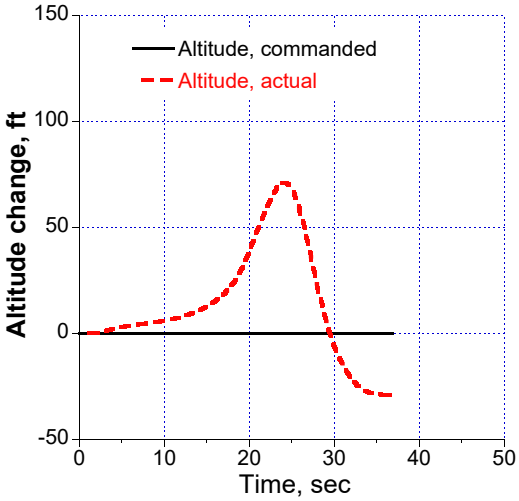

(b) 210 knot, 30 second

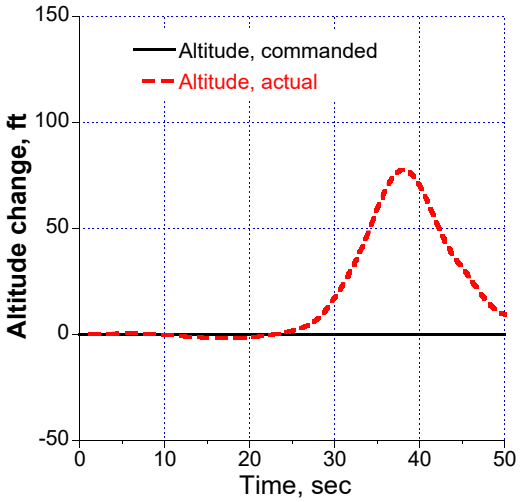

(c) 180 knot, 45 second

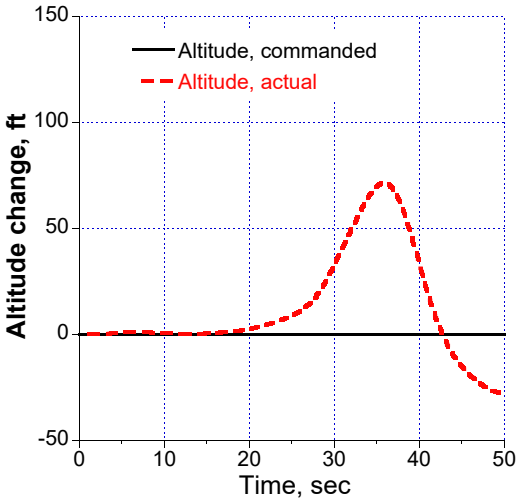

(d) 210 knot, 45 second

Fig. 8. Altitude change.

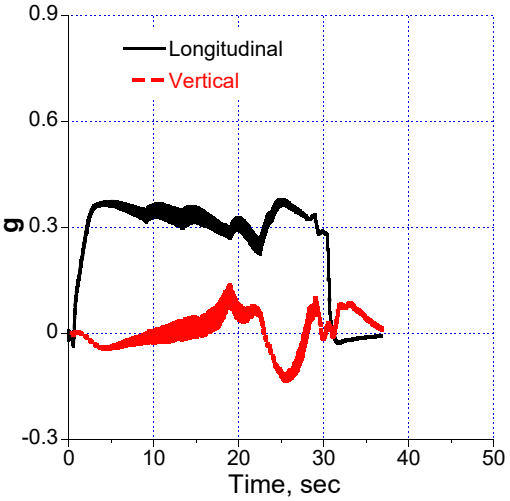

(a) 180 knot, 30 second

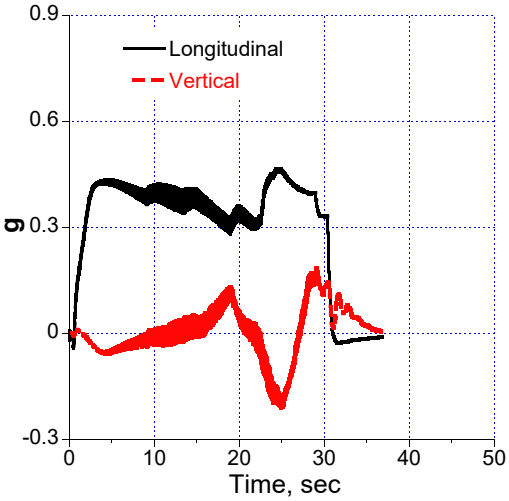

(b) 210 knot, 30 second

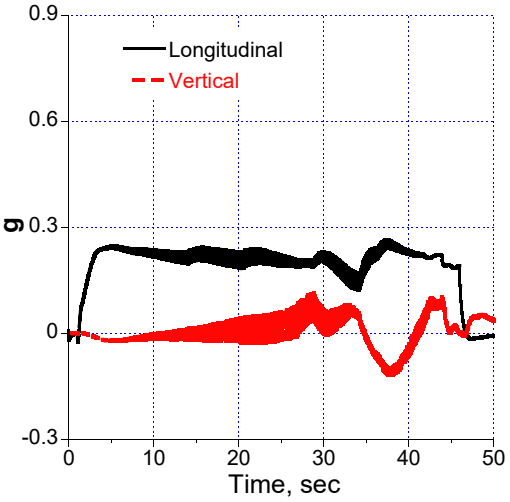

(c) 180 knot, 45 second

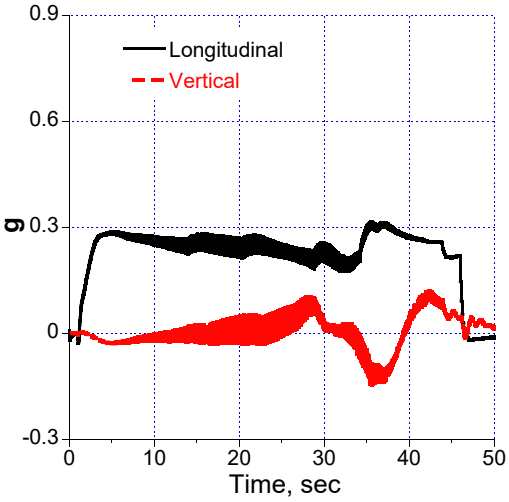

(d) 210 knot, 45 second

Fig. 9. Acceleration.

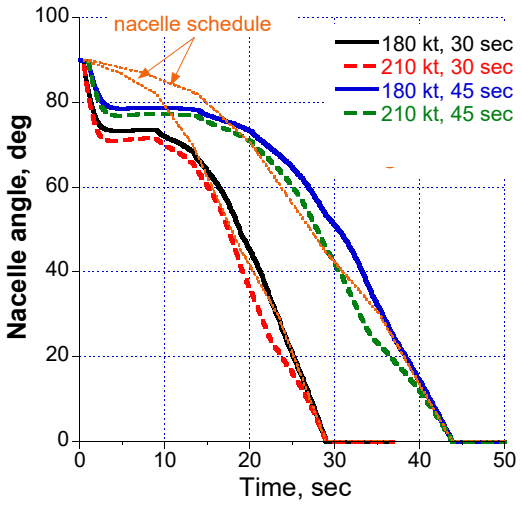

(a) Nacelle

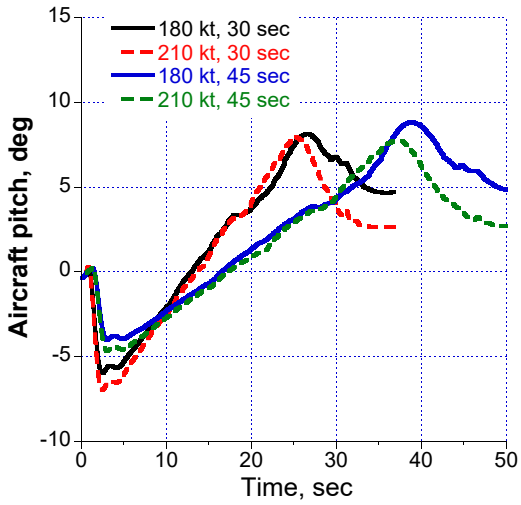

(b) Aircrft pitch

Fig. 10. Nacelle angle and aircraft pitch.

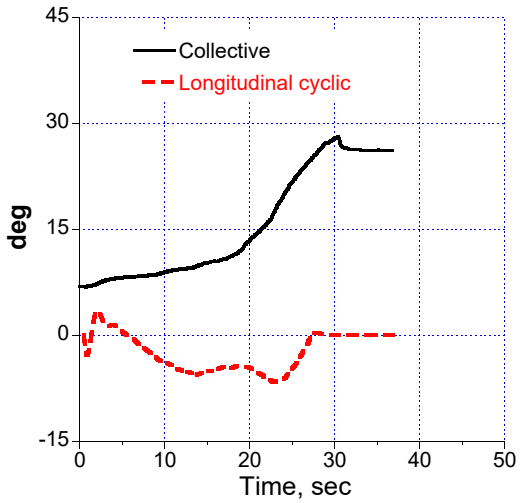

(a) 180 knot, 30 second

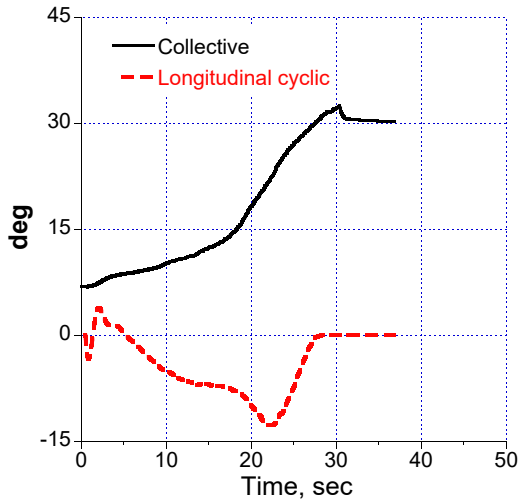

(b) 210 knot, 30 second

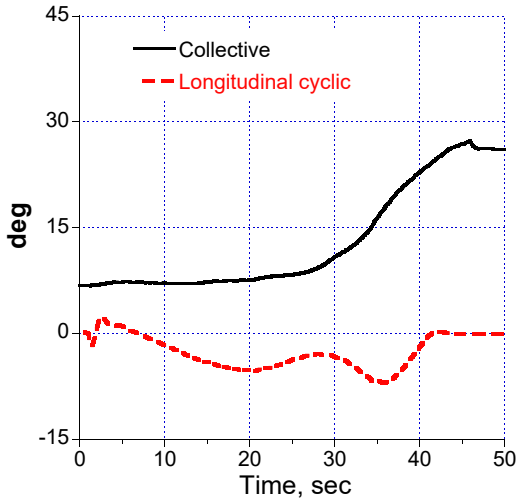

(c) 180 knot, 45 second

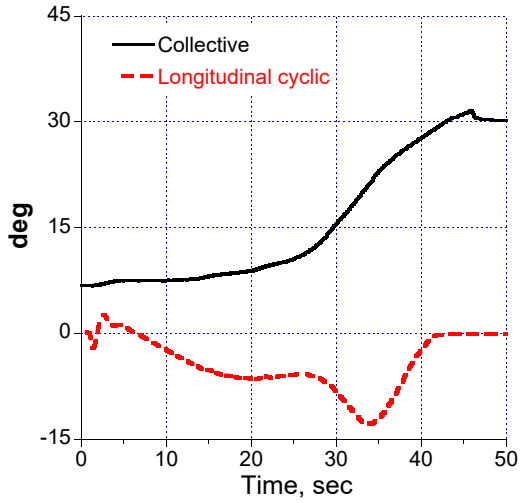

(d) 210 knot, 45 second

Fig. 11. Pilot control.

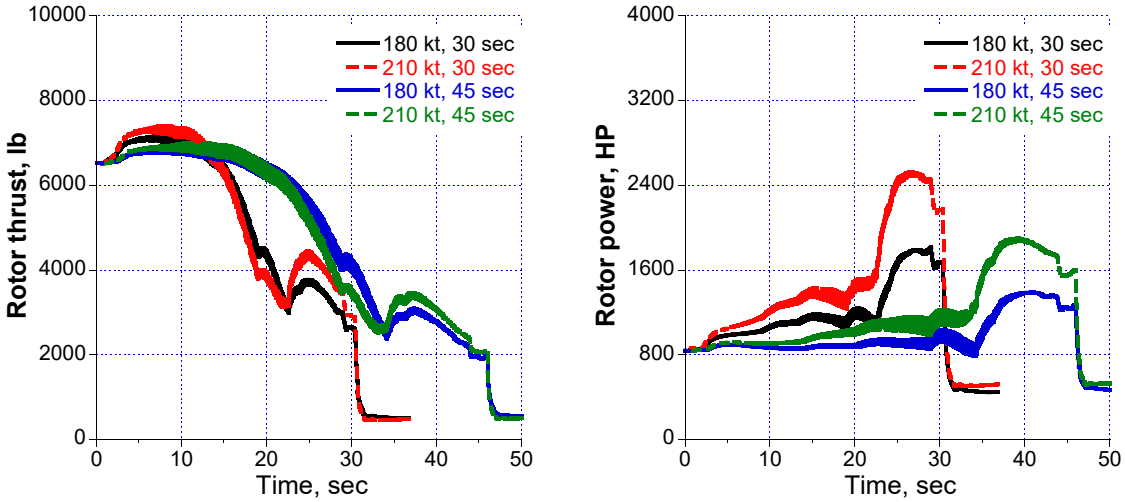

(a) Rotor thrust (b) Rotor power

Fig. 12. Rotor thrust and power.

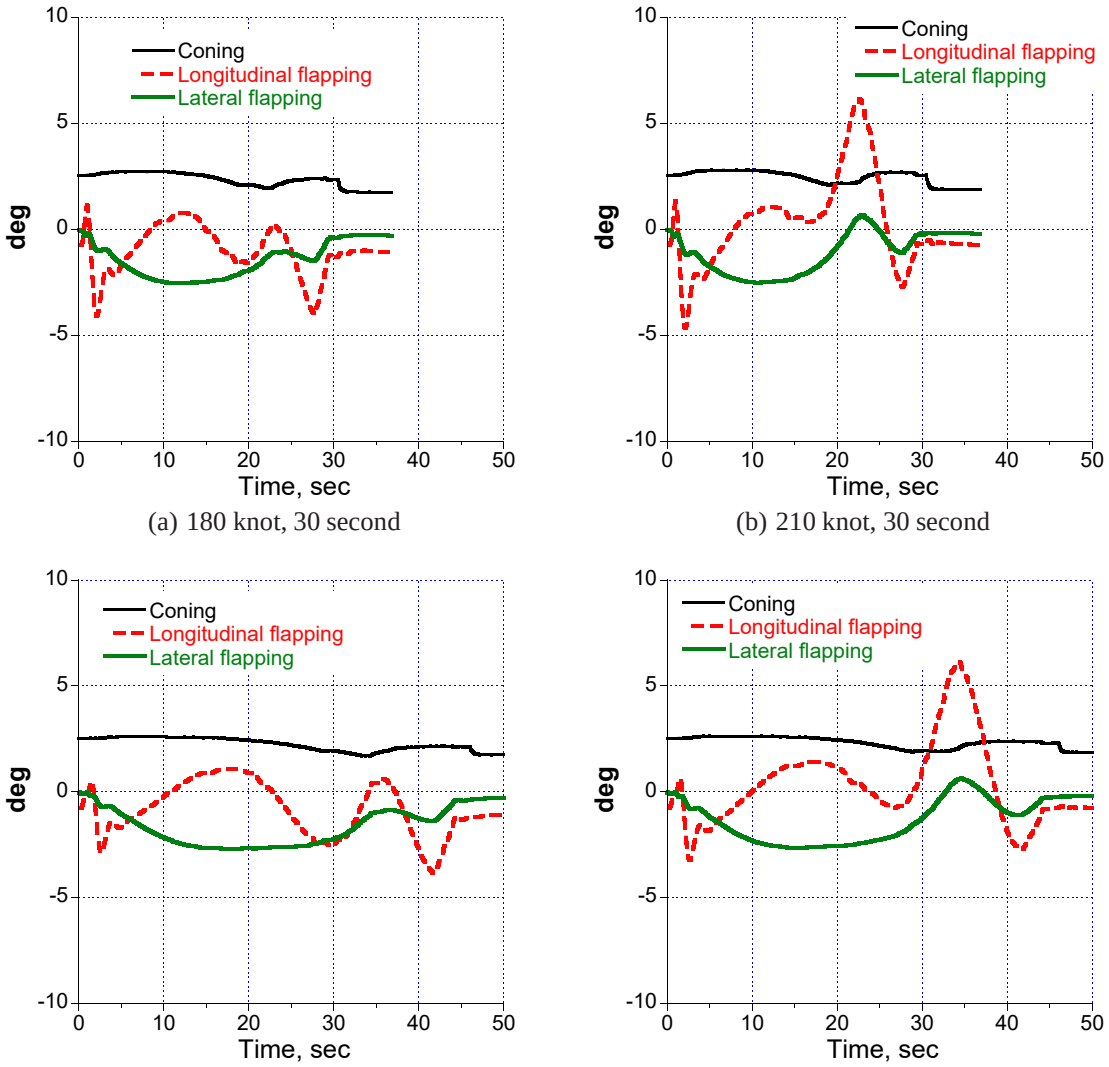

(a) 180 knot, 30 second (b) 210 knot, 30 second

(c) 180 knot, 45 second (d) 210 knot, 45 second

Fig. 13. Flap angles at the gimbal.

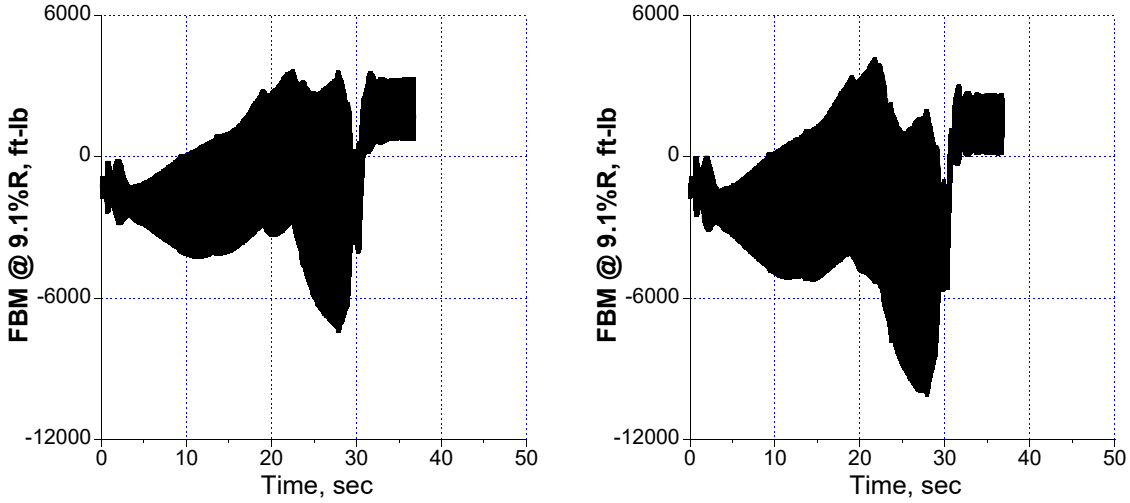

(a) 180 knot, 30 second

(b) 210 knot, 30 second

(c) 180 knot, 45 second

(d) 210 knot, 45 second

Fig. 14. Flap bending moment (FBM) at 9.1%R.

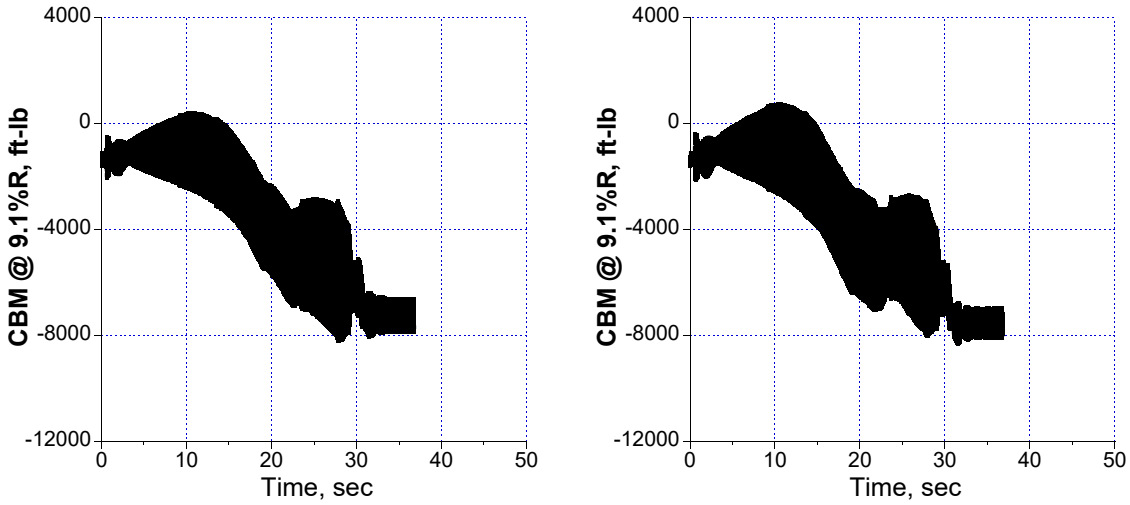

(a) 180 knot, 30 second

(b) 210 knot, 30 second

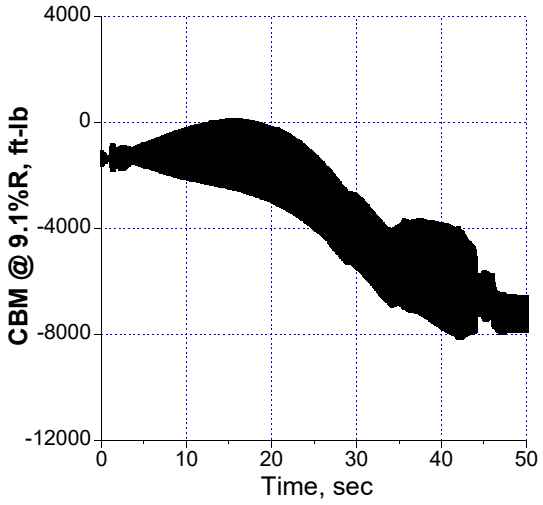

(c) 180 knot, 45 second

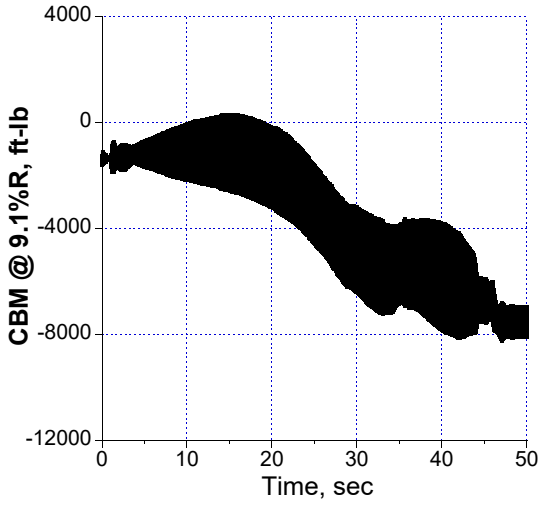

(d) 210 knot, 45 second

Fig. 15. Chord bending moment (CBM) at 9.1%R.

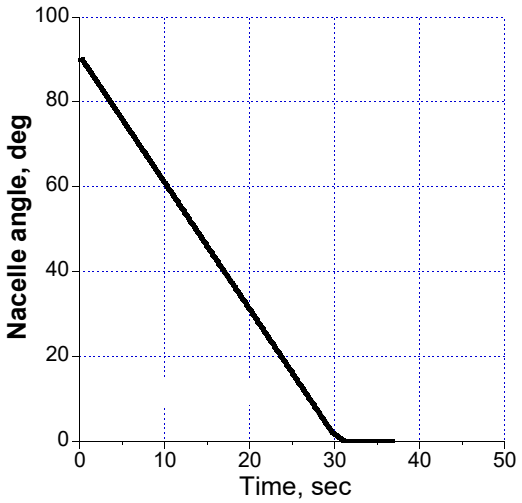

(a) Nacelle angle

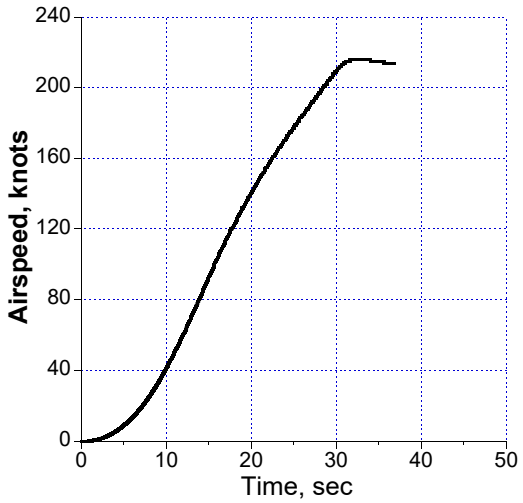

(b) Airspeed

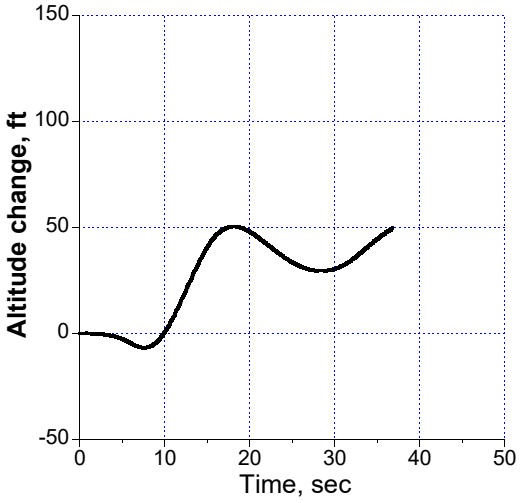

(c) Altitude change

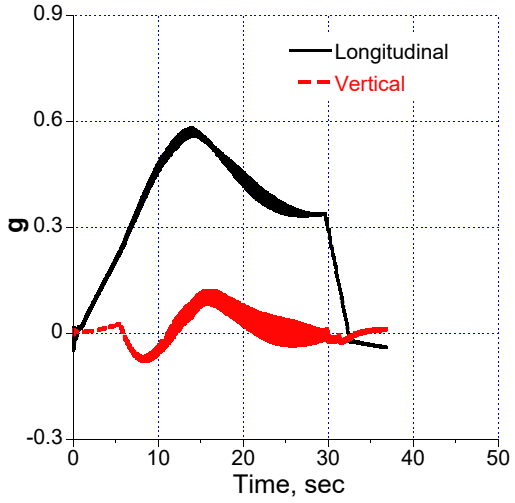

(d) Acceleration

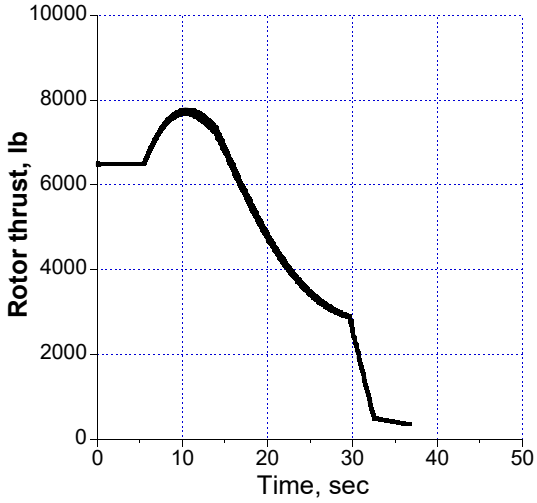

(e) Rotor thrust

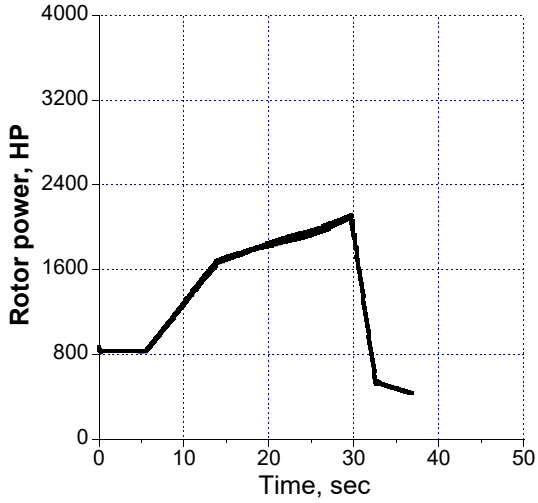

(f) Rotor power

Fig. 16. Aircraft dynamics and rotor performance with alternative conversion strategy.